Isothermal Thickening and Thinning Processes in Low Molecular Weight Poly(ethylene oxide) Fractions Crystallized from the Melt. 3. Molecular Weight Dependence

Stephen Z. D. Cheng,* Jianhua Chen, Jeffrey S. Barley, and Anqiu Zhang

Institute and Department of Polymer Science, College of Polymer Science and Polymer Engineering, University of Akron, Akron, Ohio 44325-3909

Anton Habenschuss and Paul R. Zschack

Oak Ridge National Laboratory, Oak Ridge, Tennessee 37831

Received July 12, 1991; Revised Manuscript Received November 14, 1991

ABSTRACT: The existence of nonintegral folding chain (NIF) crystals in a series of poly(ethylene oxide) (PEO) fractions with molecular weight ranging between 3000 and 23 000 has been observed through time-resolved synchrotron small-angle X-ray scattering (SAXS), differential scanning calorimetry (DSC), and transmission electron microscopy (TEM) experiments. It has been found that with increasing molecular weight the isothermal thickening and/or thinning processes which lead to formation of the final integral folding chain (IF) crystals are increasingly hampered. At sufficiently high molecular weights, NIF crystals may be permanently retained. The thermodynamic driving force for these processes is discussed. An explanation of the NIF to IF transformation consists of both a thermodynamic reason (Gibbs free energy change) and a kinetic effect (chain diffusional motion and chain fold number). Of additional interest, the fold length of initial NIF crystals increases with crystallization temperature (or decreasing supercooling) for each fraction as commonly observed in polymer lamellar crystals with a relationship of $l = C_2 + C_1/\Delta T$. However, the slope C_1 increases with molecular weight instead of remaining constant as theoretically predicted. This may be caused by a change of the fold surface free energy due to loose folds, chain ends, and hydrogen bonding in the NIF crystals.

Introduction

One of the experimental approaches to help understand polymer crystal growth is to study the crystal growth behavior of a series of pure oligomers or low molecular weight fractions and connect growth mechanisms of these smaller molecules to macromolecules. A pioneering series of studies was conducted on low molecular weight poly(ethylene oxide) (PEO) fractions by Kovacs et al.[1-5] They investigated isothermal crystal growth behavior, lamellar thickening, and crystal melting of single PEO lamellar crystals grown from the melt. The molecular weight range studied was between 2000 and 10 000. In the low supercooling region, these low molecular weight PEO fractions are in the form of integrally folded (IF) single lamellar crystals. The presence of IF crystals implies that the chain hydroxyl end groups are rejected from the crystal interior and located at the surface layers of the lamellae. It has been further observed that the folded-chain crystals in these PEO fractions are metastable with respect to the extended-chain crystals. For a given molecular weight, the number of folds (n) per molecule depends not only upon the crystallization temperature (T_c) but also upon the crystallization time (t_c). As T_c and t_c increase, the lamellar thickness increases in a stepwise manner due to the quantized reduction of n until there is full chain extension.[1-5] A parallel study was conducted by Booth's research group. Furthermore, they also synthesized a variety of different end groups such as alkoxy[6,7] and acetoxy.[8] Results similar to those for PEO fractions have been reported for these end-group modified polymers.

Nevertheless, how chain molecules behave during IF crystal formation remains an unanswered question. The first observation of nonintegral folding chain (NIF) crystals was recently reported for n-alkanes crystallized from the melt by Ungar and Keller[9,10] and solution by Organ et al.[11] In low molecular mass PEO fractions, we have also observed the existence of NIF crystals over wide crystallization temperature regions and for various molecular weights.[12-17] It is evident that the IF crystal is derived from isothermal thickening or thinning of the NIF crystal. The NIF crystal is thermodynamically the least stable state but grows the fastest. Isothermal thickening and thinning processes may occur within crystals at low crystallization temperatures or even on the crystal growth surface at high temperatures. This leads to a conclusion that in these pure oligomers and low molecular weight fractions the crystal growth is a compromise between the thermodynamic driving force and kinetic pathway.[9,17]

Since our purpose is to study the polymer crystal growth mechanism through investigation of low molecular weight PEO fractions, in this paper we attempt to understand the molecular weight effect on crystal growth behavior in these fractions. In particular, we focus on changes of the fold length of NIF crystals with isothermal crystallization temperatures, times, and fold numbers.

Experimental Section

Materials. Six low molecular weight PEO fractions were purchased from Polymer Laboratories, Ltd., as standard materials and refractionated in our laboratory. Their molecular weights are 3000, 4250, 7100, 10 500, 12 600, and 23 000, respectively, with polydispersities of 1.02, 1.03, 1.04, 1.04, 1.05, and 1.05. These PEO fractions possess hydroxyl end groups (–OH). Table I lists the melting temperature for each fraction[18,19] as well as the average chain length which was calculated from $l = \bar{M}_n/158.2$.[4]

Instrument and Experiments. In this study, time-resolved synchrotron small-angle X-ray scattering (SAXS) experiments were carried out at the Oak Ridge National Laboratory beamline, X-14, at the National Synchrotron Light Source (NSLS). X-14 is a general purpose scattering line.[20] Equipment on this line has been described in detail in the first two papers of this series. In brief, the synchrotron X-ray beam was focused through

* To whom correspondence should be addressed.

0024-9297/92/2225-1453$03.00/0

Table I
Molecular Characterizations and Melting Temperatures of Six PEO Fractions

mol wt ($\bar{M}_n$)	polydispersity ($\bar{M}_w/\bar{M}_n$)	av chain length, nm	T_m, °C
3 000	1.02	18.9	58.7
4 250	1.03	26.9	61.1
7 100	1.04	44.9	64.0
10 500	1.04	66.4	65.4
12 600	1.05	79.6	65.6
23 000	1.05	145.4	67.0

a dynamically bent S_i crystal monochromator with a beam size of 0.1 × 1.0 mm (VXH) at the sample position. The X-ray wavelength was 1.5498 Å controlled through the monochromator set at 8.000 keV. A position-sensitive proportional counter (PSPC, Ordella 1020) was used to record the scattering pattern. A Mettler hot stage (FP-52) was situated on a Huber goniometer with the PSPC for isothermal experiments. The temperature was calibrated with standard melting materials during the beam radiation, and the precision of control was ±0.5 °C. The minimum time between placement of the sample in the hot stage and the start of data collection was approximately 0.9 min. Lorentz correction was made by multiplying the intensity, I (counts per second), with s^2 ($s = 2 \sin(\theta/\lambda)$, where λ is the wavelength of the synchrotron X-ray). For low molecular weight PEO fractions, crystallinities approach 100% even for the highest molecular weight fraction (MW = 23 000) studied (about 95%).[21] Therefore, the long spacings observed by SAXS were assumed to be representative of the lamellar crystal fold length without further correction.

PEO fractions of about 40 mg each were placed in rectangular aluminum cups and heated to 30 °C above their melting temperatures (Table I). The specimens were then quickly quenched to 40 °C where crystallization occurs rapidly. They were reheated very slowly at a heating rate of 0.1 °C/min to a self-seeding temperature, T_s, 0.5 °C lower than the melting temperature and held isothermally for 20 min. At this point in time, most of the material was molten except for a very small amount of extended-chain crystal produced through the previous quenching. The specimens were then quickly moved to another hot stage at a predetermined crystallization temperature for isothermal experiments. This self-seeding technique was previously used by Kovacs et al.[1] and is a very reproducible procedure. SAXS measurements began at 0.9 min after sample switching.

Differential scanning calorimetry (DSC) measurements were carried out on a TA thermal analysis system 9000. The DSC was calibrated in both temperature and heat flow scales at different heating rates (0.5–80 °C/min) using standard materials. The same self-seeding procedure was applied as in the SAXS experiments prior to isothermal crystallization. Successive heating scans follow without prior cooling after the complete crystallization of the samples (about 6 times longer than the exothermic crystallization peak time).

Transmission electron microscopy (TEM) experiments were also conducted on the PEO fractions in order to determine the lamellar thickness of the crystals independently. The PEO samples were crystallized by the same procedure as for SAXS and DSC, followed by surface replication using heavy metal (Au/Pt, 40/60) and carbon. The detailed procedure has been described in ref 22. A JEOL JEM-120U transmission electron microscope with a 100-kV accelerating voltage was used in this study.

Results

Existence of NIF Crystals. Figures 1–4 show time-resolved synchrotron SAXS data for four PEO fractions with different molecular weights of MW = 3000, 10 500, 12 600, and 23 000 at crystallization temperatures of 46, 50, 50, and 54 °C, respectively. For the PEO (MW=3000) fraction (Figure 1), a scattering peak with a fold length of 13.1 nm is clearly observed at $t_c = 1.4$ min. With increasing crystallization time, this scattering peak intensity decreases, and two other scattering peaks at 19.0 and 10.0 nm gradually develop. At t_c = 11.4 min, the initial

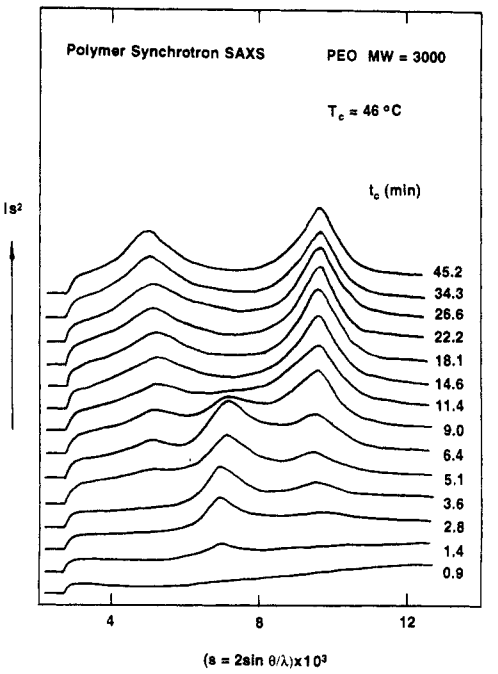

Figure 1. Set of time-resolved synchrotron SAXS data for PEO-(MW=3000) crystallized at 46 °C.

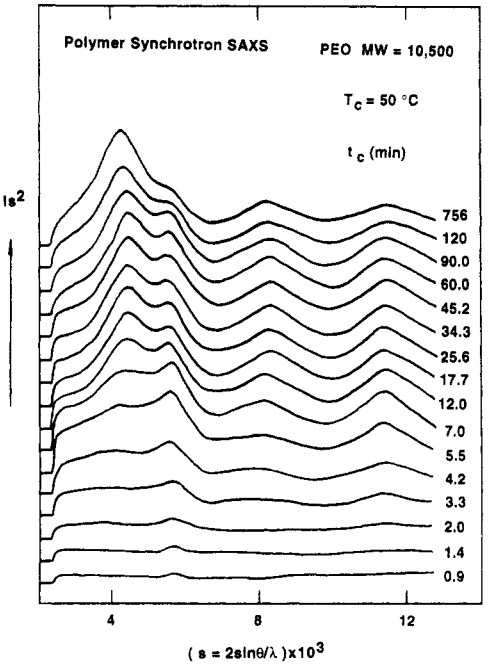

Figure 2. Synchrotron SAXS data for PEO(MW=10 500) crystallized at 50 °C.

scattering peak has almost totally disappeared and the peak at 10.0 nm has become the dominant scattering peak with another small scattering peak at 19.0 nm. Since the fold lengths of 19.0 and 10.0 nm correspond to those of the IF(n=0) and IF(n=1) crystals, respectively, the initial scattering peak of 13.1 nm is recognized as an NIF crystal.

With increasing molecular weight, the SAXS pattern becomes increasingly complicated since multiple IF crystals may coexist. For the PEO(MW=4250) and PEO-(MW=7100) fractions, the synchrotron SAXS results have been reported in the first and second parts of this series.[16,17] Figure 2 shows the results for the PEO(MW=10 500) fraction crystallized at 50 °C. At $t_c = 0.9$ min, a fold length of 18.1 nm can be observed. This fold length exists in all the SAXS curves within the experimental time scale.

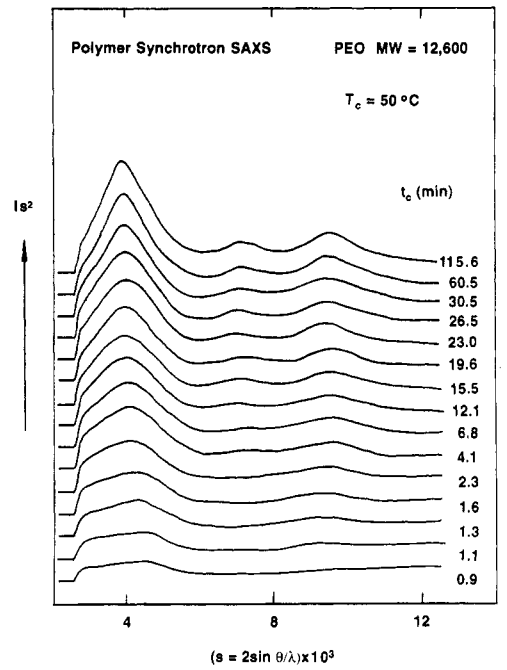

Figure 3. Synchrotron SAXS data for PEO(MW=12 600) crystallized at 50 °C.

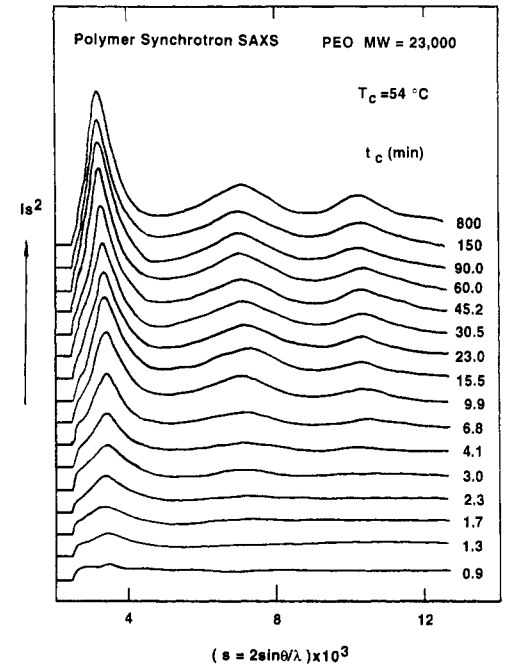

Figure 4. Synchrotron SAXS data for PEO(MW=23 000) crystallized at 54 °C.

However, the intensity of this fold length increases first and then decreases at a longer time. On the other hand, a new scattering peak at 22.0 nm appears at t_c = 4.2 min and grows monotonically with increasing time. Note that a twice-folded chain crystal for this fraction possesses a fold length of 22.1 nm. An isothermal thickening process is thus evident in this case. Two other weak scattering peaks at 11.5 and 8.9 nm may be the second-order scattering of the previous two peaks of 22.0 and 18.1 nm (in particular, their intensity developments closely correspond to the scattering peaks at 22.0 and 18.1 nm, and their ratios are all close to constant for each pair of scattering peaks). Figure 3 shows the SAXS data for the molecular weight increased to 12 600 and crystallized at 50 °C. At t_c = 0.9 min, a broad scattering peak centered

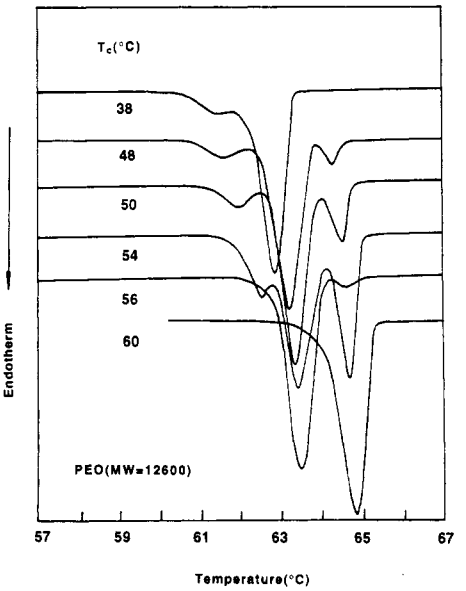

Figure 5. DSC heating traces for the PEO(MW=12 600) fraction crystallized at different temperatures (heating rate 0.5 °C/min).

at 22.7 nm can be identified. With increasing time, the intensity of this peak grows and the peak position gradually shifts toward 26.0 nm at t_c = 115.6 min. This fold length is still about 0.5 nm shorter than the fold length of IF(n=2) crystals for this fraction, 26.5 nm. At a long enough crystallization time one would expect that the fold length of this NIF crystal may finally stabilize at the fold length of the IF(n=2) crystal.

A similar isothermal thickening process can be observed in the case of PEO(MW=23 000) crystallized at T_c = 54 °C, as shown in Figure 4. A gradual but continuous increase of the fold length with time can be seen. However, in this case the fold length of the NIF crystal (28.4 nm) lies between IF(n=4) and IF(n=5) crystals. Their corresponding fold lengths are 29.1 and 24.1 nm, respectively.

Differential scanning calorimetry (DSC) measurements for the completely crystallized PEO(MW=12 600) fraction are given in Figure 5. It is evident that at low crystallization temperatures below 42 °C, two melting peaks can be observed: one main peak at 62.5–63.5 °C and a small shoulder around 61–62 °C. Starting at T_c = 42 °C, three melting peaks appear. The highest melting peak at 64–65 °C gradually develops with increasing crystallization temperature. Surprisingly enough, at T_c = 56 °C this high melting peak suddenly almost disappears. This is similar to the cases of PEO(MW=4250) and PEO(MW=7100) where abnormal crystal melting behavior was found.[16,17] Further increasing the crystallization temperature to 57 °C gives rise to a major melting peak at 64.3 °C. This peak corresponds to the high melting peak, which was observed at T_c = 54 °C and almost disappeared at T_c = 56 °C. At even higher crystallization temperatures, only one high melting peak exists; it is in the vicinity of 65 °C. A slight increase of this melting temperature to 65.7 °C can also be found when the crystallization temperature is further increased.

Figures 6 and 7 show relationships between the melting and crystallization temperatures for both the PEO(MW=12 600) and PEO(MW=23 000) fractions. In each case it is clear that below a certain crystallization temperature only two melting peaks can be observed. Above that, multiple peaks exist. In particular, for the PEO(MW=23 000) between T_c = 50 and 56 °C, as many as four melting peaks are evident. Their heats of fusion vary with crystallization temperature. Furthermore, only one melt-

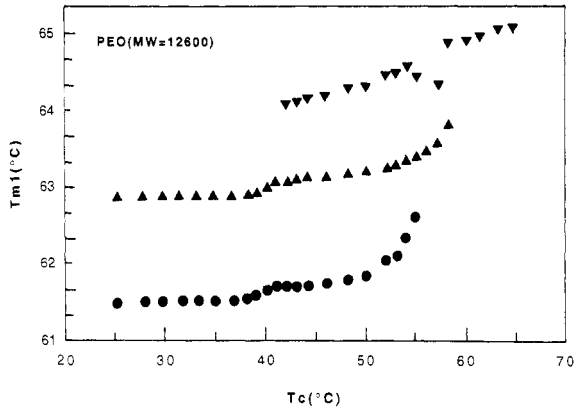

Figure 6. Relationships between the melting and crystallization temperatures for the PEO(MW=12 600) fraction.

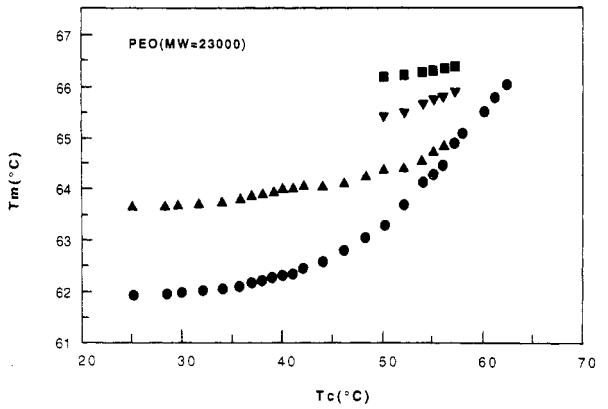

Figure 7. Relationships between the melting and crystallization temperatures for the PEO(MW=23 000) fraction.

ing temperature peak displays significant T_c dependence, with the others relatively independent of T_c. These T_c-dependent melting peaks are associated with NIF crystals (see below). For the PEO(MW=23 000) fraction, above T_c = 57 °C, the high melting peaks disappear. Only one peak remains, corresponding to the continuous increase of T_m. Further increasing T_c does not bring back the high melting peaks.

Changes of NIF Crystal Fold Lengths with Temperature and Molecular Weight. Figures 8 and 9 are relationships between the fold length (lamellar thickness) and crystallization temperature for two fractions (MW = 3000 and 7100). The data in these figures are from observations of both SAXS (points) and TEM (bars). It is clear that, besides the fold lengths of the IF crystals, a NIF crystal exists, and its fold length increases continuously with crystallization temperature. For the PEO(MW=3000) fraction, the fold length of the NIF crystal is always in between those of the IF(n=1) and IF(n=0) crystals. However, for the case of the PEO(MW=7100) fraction the fold length of the NIF crystal is in between the IF(n=2) and IF(n=1) crystals below T_c = 52 °C and in between the IF(n=1) and IF(n=0) crystals above T_c = 52 °C. In the vicinity of T_c = 52 °C, the fold length of the NIF crystal is approximately the same as that of the IF(n=1) crystal.

Figure 10 summarizes the fold length changes of the initial NIF crystals for six PEO fractions with reciprocal supercooling (supercooling $\Delta T = T_m - T_c$; T_m in Table I). The data of PEO(MW=4250) and PEO(MW=7100) fractions are taken from refs 16 and 17, and the others are new results reported in this work. It is interesting that for each fraction the fold length increases linearly with reciprocal ΔT. Furthermore, the slope of these lines

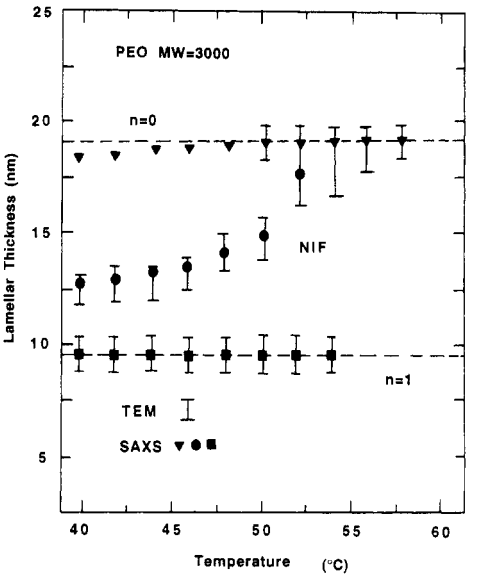

Figure 8. Relationships between the fold length (lamellar thickness) and crystallization temperature for PEO(MW=3000).

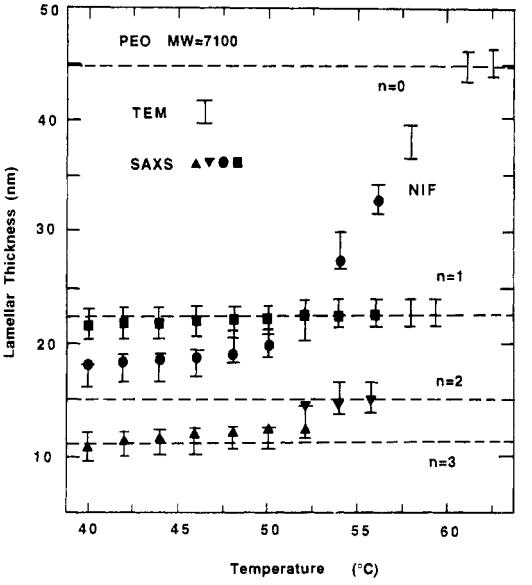

Figure 9. Relationships the same as those in Figure 8 for PEO(MW=7100).

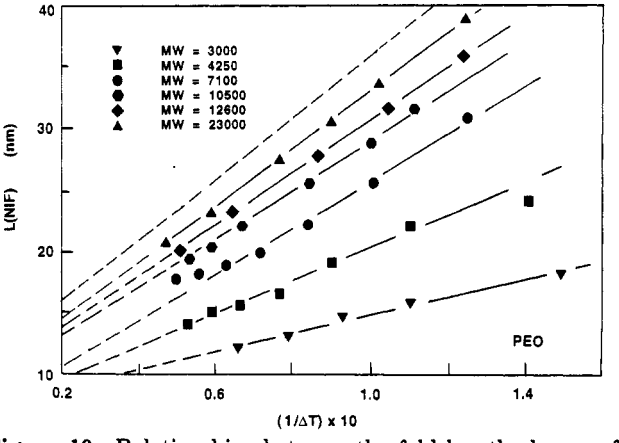

Figure 10. Relationships between the fold length change of NIF crystals and reciprocal supercooling.

increases with the molecular weight. Nevertheless, the intercepts are almost constant at around 6.5–8.0 nm. It has been found that the fold length of NIF crystals shows a linear relationship with the reciprocal of the molecular

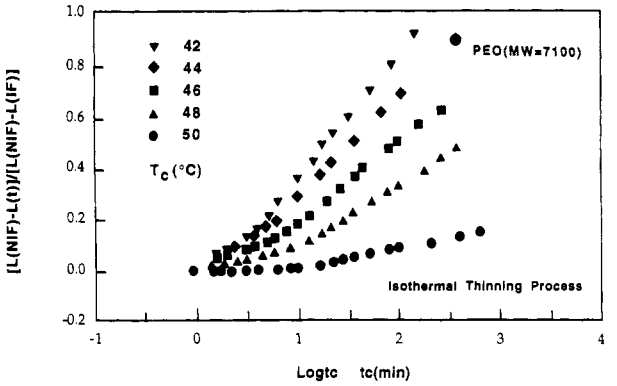

Figure 11. Ratio of $\Delta l/\Delta l_0$ (for the definition, see text) changes with respect to log t_c at different temperatures (T_c) for the isothermal thinning process of PEO(MW=7100).

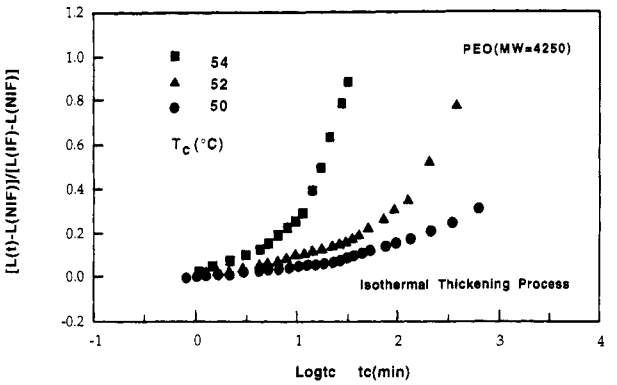

Figure 12. Relationships the same as those in Figure 11 for the isothermal thickening process of PEO(MW=4250). Note that the ratios are greater than zero because of the denominator of L(IF) − L(NIF) instead of L(NIF) − L(IF).

weight at constant supercooling. One can thus extrapolate the reciprocal molecular weight to zero (molecular weight to infinity) to obtain the fold length of NIF crystals of an infinitely long chain length. The dashed line in Figure 10 represents these extrapolated data; a linear relationship with a slope of 270 nm °C and an intercept of 8.5 nm is found.

Changes of NIF Crystal Fold Length with Time. In order to study the kinetics of isothermal thickening and thinning processes for different molecular weight PEO fractions, a comparison of the kinetics at a constant reference must be made. We define a ratio of $[L(\text{NIF}) - L(t)]/[L(\text{NIF}) - \text{L(IF)}] = \Delta l/\Delta l_0$ to represent the change of the NIF crystal fold length with time, where $L(t)$ is the fold length at time t, L(NIF) is the fold length of the initial NIF crystal, and L(IF) is the fold length of the final IF crystal reached through either isothermal thickening or thinning. This ratio indicates the percentage of the fold length change relative to the total difference between the initial and the final states.

Figure 11 shows the ratio of $\Delta l/\Delta l_0$ change with respect to log t_c at different crystallization temperatures for the isothermal thinning process of the PEO(MW=7100) fraction. Two-step changes of the ratio values can be identified and correspond to the thinning process during and after crystallization, respectively.[16,17] It is evident that the slope ($\text{d}(\Delta l/\Delta l_0)/\text{d log } t_c$) of the second step in Figure 11 decreases with increasing isothermal crystallization temperature. This indicates that with increasing temperature the isothermal thinning process slows down. On the other hand, a similar relationship can be plotted for the isothermal thickening. It is shown in Figure 12 for PEO(MW=4250) as an example. For isothermal thickening, the slope of the second step increases with the crystallization temperature. Table II lists the slope data of isothermal thickening and thinning processes for each PEO fraction at different crystallization temperature. It is clear that the rate of the transition kinetics is reduced by the increase of the chain length and/or fold number.

Table II
Slopes of Isothermal Thickening and Thinning Processes for Different PEO Fractions

MW	T_c, °C	$\text{d}(\Delta l/\Delta l_0)/\text{d log } t_c$
3 000	46	0.61 [thickening to IF(n=0)]
	48	1.22 [thickening to IF(n=0)]
4 250	42	0.69 [thinning to IF(n=1)]
	44	0.48 [thinning to IF(n=1)]
	46	0.44 [thinning to IF(n=1)]
	48	0.41 [thinning to IF(n=1)]
	50	0.42 [thickening to IF(n=0)]
	52	0.87 [thickening to IF(n=0)]
	54	2.06 [thickening to IF(n=0)]
7 100	42	0.43 [thinning to IF(n=2)]
	44	0.41 [thinning to IF(n=2)]
	46	0.34 [thinning to IF(n=2)]
	54	0.68 [thinning to IF(n=1)]
	56	0.47 [thinning to IF(n=1)]
	44	0.46 [thickening to IF(n=1)]
10 500	50	0.31 [thinning to IF(n=2)]
	56	0.41 [thinning to IF(n=1)]
	46	0.30 [thickening to IF(n=2)]
12 600	50	0.25 [thickening to IF(n=2)]
	56	0.32 [thickening to IF(n=1)]
23 000	50	0.11 [thickening to IF(n=5)]
	54	0.12 [thickening to IF(n=4)]

Discussion

This is perhaps the first opportunity to investigate the crystal growth behavior of NIF crystals in a systemic manner through a series of low molecular weight PEO fractions. The significance of this study is not only to understand the crystal growth mechanism of these fractions but also to extend our knowledge of polymer crystal growth. Our discussion focuses on three aspects:

1. What is the thermodynamic driving force of the isothermal thickening and thinning processes?

2. How seriously is the thickening or thinning process hampered with increasing molecular weight and chain fold number?

3. Can we find a correlation between the NIF crystal growth in the low molecular weight PEO fractions and high molecular weight PEO crystal growth?

The experimental evidence from SAXS (Figures 1–4), DSC (Figures 5–7), and TEM (Figures 8 and 9) should leave little doubt about the existence of NIF crystals in low molecular weight PEO fractions. From LAM Raman spectroscopy, Krimm's group has also found these NIF crystals (which they designated "fractional IF crystals") in low molecular weight PEO fractions.[24] In particular, the DSC results indicate that only one melting peak has a large T_c dependence (the lowest one). This melting peak corresponds to the NIF crystal. Other higher melting peaks resulted from annealing and perfection (through thickening and/or thinning) during heating. However, the isothermal thinning process may still be a puzzle since a tilted chain molecule will form a lamellar crystal of smaller thickness but with the same fold length. A decrease of the lamellar thickness may possibly be caused by some kind of tilting process rather than a shortening of the fold length. In the low molecular weight PEO fractions the NIF crystals crystallized first, and the overall crystallization at low crystallization temperatures ends after only a few minutes.[12,13,16,17] Therefore, further thickness changes

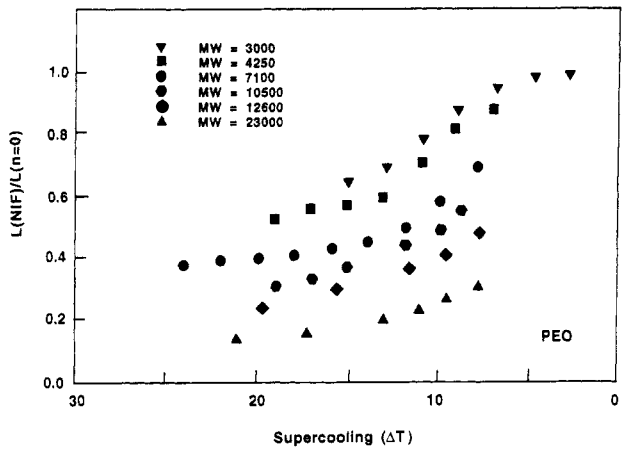

Figure 13. Relationships between the ratio of $L(\mathrm{NIF})/L(n=0)$ and supercooling for six PEO fractions with different molecular weights.

observed from SAXS basically occur in the solid state through annealing and perfection. The tilting process in the solid state, if it happens, needs a large amount of molecular cooperative motion in the crystals as well as an extra formation volume to allow this kind of motion. On the other hand, the isothermal thinning process is pronounced in the low crystallization temperature region where the NIF crystals are thermodynamically less stable than the IF crystals (see below).

To explain the isothermal thickening and thinning processes, both thermodynamic and kinetic effects need to be taken into account. The thermodynamic stability of the crystal can be represented by its Gibbs free energy, G_c. The fold length of the lamellar crystal is L. Two possibilities exist. The first case is that the NIF crystal is the least stable crystal, but its fold length is in between those of two sequential IF crystals:

$$G_c(\mathrm{NIF}) > G_c(\mathrm{IF},n=i+1) > G_c(\mathrm{IF},n=i) \quad (1)$$

and

$$L(\mathrm{IF},n=i) > L(\mathrm{NIF}) > L(\mathrm{IF},n=i+1) \quad (2)$$

where $i = 0, 1, 2, \ldots$. Therefore, isothermal thickening may occur through $L(\mathrm{NIF})$ toward $L(\mathrm{IF},n=i)$ or isothermal thinning through $L(\mathrm{NIF})$ toward $L(\mathrm{IF},n=i+1)$.

The second case is that in which both the thermodynamic stability and fold length are in between those of two neighboring IF crystals:

$$G_c(\mathrm{IF},n=i+1) > G_c(\mathrm{NIF}) > G_c(\mathrm{IF},n=i) \quad (3)$$

and

$$L(\mathrm{IF},n=i) > L(\mathrm{NIF}) > L(\mathrm{IF},n=i+1) \quad (4)$$

Isothermal thinning is thus forbidden, and only the isothermal thickening process can take place. Equations 3 and 4 represent a common observation of polymer lamellar crystals that lamellar thickness is proportional to thermodynamic stability.

Two conditions allow the first case (eqs 1 and 2) to be included. First, chain end defects may be included within the crystal interior. Second, the lamellar crystal surfaces for the NIF crystals may be very irregular and rough due to loose folds and cilia. Both effects reduce the thermodynamic stability of the NIF crystal, allowing the condition described by eq 1 to exist.

Either of the observed thickening and thinning processes must involve chain molecular motion and in particular diffusional motion along the crystallographic c-axis. At low crystallization temperatures (say, $\Delta T > 12$ °C) such motion occurs within the crystals, while at high crystallization temperatures the motion may also take place on the growing surface. This molecular diffusional motion depends not only on how many repeating units move together but also on the fold number per chain molecule in the initial NIF state. The former may be described by means of an energy term needed for such motion $\xi\nu d$, where ξ is the friction coefficient per repeat unit, ν is the number of repeat units moving together, and d is the distance for the motion. If one considers the fold number effect as in the latter case, the motion may involve two or more chain stems moving simultaneously and exhibits a cooperative nature. Determination of a quantitative description of this phenomenon is still under investigation. One may expect that an activation energy of the diffusional motion, E_r, could be helpful. Phillips and Rensch reported such an activation energy for thickening in low molecular weight poly(ϵ-caprolactone) to be 418 kJ/mol.[23] Since this energy can break a single carbon–carbon covalent bond, one must conclude that it represents a cooperative motion.

Therefore, the Gibbs free energy change during the thickening or thinning is

$$\Delta G = \Delta G(\mathrm{NIF}\rightarrow\mathrm{IF}) + E_r \quad (5)$$

where $\Delta G(\mathrm{NIF}\rightarrow\mathrm{IF})$ represents the difference between the Gibbs free energies of the initial NIF crystal and of the final IF crystal. This term is negative as indicated in eqs 1 and 3, in contrast with the activation term E_r, which is positive. Which process will occur faster, either thickening or thinning, thus depends upon the compromise between the thermodynamic contribution and the kinetic effect. With increasing molecular weight, one expects that the difference between $G_c(\mathrm{NIF})$ and $G_c(\mathrm{IF})$ decreases. On the other hand, E_r increases due to increasingly large-scale cooperative motion (in particular due to the increasing fold number). As a result, the thermodynamic driving force quickly vanishes and the fold length of NIF crystals may remain as a permanent state with only local isothermal thickening as in the case for most high molecular weight polymer crystals.

Turning to a discussion of the results shown in Figure 10, it is evident that the fold length of NIF crystals has a linear relationship with the reciprocal of the supercooling (ΔT):

$$L(\mathrm{NIF}) = C_2 + C_1/\Delta T \quad (6)$$

This relationship has been predicted by nucleaton theory[25-29]

$$l_g^* = \frac{2\sigma_e T_m}{\Delta h_f \Delta T} + \frac{kT}{b_0\sigma} = \frac{2\sigma_e T_m}{\Delta h_f \Delta T} + \delta \quad (7)$$

where l_g^* is the initial lamellar thickness (or more precisely the length of the stems between the two fold surfaces) and Δh_f and T_m are the equilibrium heat of fusion and melting temperature, respectively. σ_e represents a fold surface free energy, while σ is a lateral surface free energy. b_0 is the thickness of one chain monolayer along the crystal growth direction, and k is the Boltzmann constant. In the case of low molecular weight PEO fractions, it has been predicted that IF crystals may be developed through NIF crystals.[28,30,31] Our experimental observations have qualitatively verified this prediction. Nevertheless, a quantitative description is more complicated by the fact that the fold length of each fraction at constant supercooling is not a constant, but rather it increases with molecular weight (Figure 10).

Table III
Different Fold Lengths of IF Crystals of Six PEO Fractions

	fold lengths, nm										
mol wt	$n = 0$	$n = 1$	$n = 2$	$n = 3$	$n = 4$	$n = 5$	$n = 6$	$n = 7$	$n = 8$	$n = 9$	$n = 10$
3 000	19.0	9.5									
4 250	26.9	13.4	(9.0)								
7 100	44.9	22.4	15.0	11.2	(9.0)						
10 500	66.4	33.2	22.1	16.6	13.3	11.1	9.5	(8.3)			
12 600	79.6	39.8	26.5	19.9	15.9	13.3	11.4	10.0	(8.8)		
23 000	145.4	72.7	48.5	36.3	29.1	24.2	20.8	18.2	16.1	14.5	13.2

If one assumes that the fold lengths of NIF crystals are representative of l_g^*, σ values can be calculated from their intercepts, which all indicate a value of around 6.5–8.0 nm. In the more elaborate and more accurate approximations that permit fluctuations of the fold length,[32] δ is roughly 1.5 times larger than $kT/(b_0\sigma)$. In the temperature range from −67 (the glass transition temperature of PEO) to 70 °C, the σ value varies between 1.0 and 2.0 erg/cm^2. Calculations based on eq 7 alone yield a σ value between 0.8 and 1.5 erg/cm^2 in the same temperature range. This value is surprisingly lower than that of other polymers such as polyethylene ($\sigma \cong 12$ erg/cm^2).[26,33] However, this value is very close to that derived from the extended-chain crystal growth kinetics of low molecular weight PEO fractions.[34] This may be an indication that the lateral surface free energies for the NIF and IF crystal growths are not very much different. On the other hand, one can calculate the fold surface free energy from the slopes of these linear relationships. Since the slope increases with molecular weight, the fold surface free energy correspondingly increases. It should be noted that the melting temperature and heat of fusion used here should also be those of the NIF crystals. Nevertheless, we found that a change in the melting temperature does not significantly vary the calculated σ_e values. Yet, the decrease of the heat of fusion of NIF crystals with molecular weight gives rise to a larger difference of σ_e for PEO(MW=3000) and PEO(MW=23 000) fractions mainly by decreasing the σ_e of PEO(MW=3000). A detailed calculation leads to a σ_e value of 31 erg/cm^2 for PEO(MW=3000) and $\sigma_e = 93$ erg/cm^2 for a PEO with infinite chain length. σ_e values of the other fractions lie correspondingly in between these two values: $\sigma_e = 50$ erg/cm^2 for PEO(MW=4250), $\sigma_e = 69$ erg/cm^2 for PEO(MW=7100), $\sigma_e = 73$ erg/cm^2 for PEO(MW=10 500), $\sigma_e = 76$ erg/cm^2 for PEO(MW=12 600), and $\sigma_e = 86$ erg/cm^2 for PEO(MW=23 000). This is similar to the case of low molecular weight polyethylene fractions. One may treat the observed fold surface free energy as the summation of the effects of cilia and folds.[26,33] In the present case, any hydrogen-bonding contribution needs to be included. Hence, the cause for the changing slope in Figure 10 may be attributed to the variation of fold surface free energy. However, the true value of l_g^* is experimentally undetermined. A very short-time synchrotron SAXS may provide further experimental evidence. These kinds of SAXS observations in polyethylene have recently been reported.[35] The lack of true l_g^* may introduce some error in the calculation of surface free energies σ and σ_e. The different forms of the crystals grown from the melt (the NIF or the IF crystals) may also lead to the variation between the σ_e data reported here and others.[3,28]

From Figures 8 and 9, one can qualitatively observe the molecular weight effect on isothermal thickening and thinning processes. However, quantitative separation of the effect of the diffusional molecular motion and the number of chain folds is difficult. This is due to the fact not only that at constant supercooling the fold number in NIF crystals increases with molecular weight but also that the friction coefficient and cooperative molecular motion is temperature-dependent instead of supercooling-dependent.

Experimentally, isothermal thickening and thinning processes are observed by a change in the fold length of the initially formed NIF crystal to that of either of the two nearest sequential IF crystals. It is certainly important to look closely at the differences between these fold lengths since they are associated with the different thermodynamic states of those crystals. Table III gives all the possible fold lengths of IF crystals for these fractions. It is clear that with increasing molecular weight the difference between the sequential fold lengths of IF crystals which result from the initial NIF crystals decreases. For example, this difference is 13.5 nm for PEO(MW=4250) between the fold length of IF(n=0) and IF(n=1) crystals, while for PEO(MW=7100), it decreases to 7.4 nm which is in between the IF(n=1) and IF(n=2) crystals. Further increasing the molecular weight leads to 5.5 nm for the PEO(MW=10 500) fraction (between IF(n=2) and IF(n=3) crystals), 4.0 nm for the PEO(MW=12 600) fraction (between IF(n=3) and IF(n=4) crystals), and 3.4 nm for the PEO(MW=23 000) fraction (between IF(n=5) and IF(n=6) crystal). This difference between the fold lengths of two neighboring IF crystals will become vanishingly small at higher molecular weights. This indicates that the isothermal thickening or thinning process slows down with increasing molecular weight. This is due to the decrease of the difference in Gibbs free energies between the initial and final states, if one expects that the thermodynamic stability of the lamellar crystal is proportional to its thickness when the molecular weight is sufficiently high. As a result, the NIF crystal fold length will remain nearly constant. This is perhaps why the fold length of the polymer lamellar crystal shows a continuous increase with crystallization temperature.

When the continuous change of the fold length from NIF to IF crystals is observed, one can compare absolute values of the slopes as listed in Table II by including the molecular weight and the fold number differences. In the case of the same fold number with different molecular weights, for example, comparing the thinning processes of PEO(MW=4250) at 42 and 44 °C with those of PEO(MW=7100) at 54 and 56 °C, the absolute values of the slopes for thinning from NIF to IF(n=1) crystals are only slightly lower for those of the PEO(MW=4250) fractions. Further comparison can also be made for the thinning processes of PEO(MW=10 500) and PEO(MW=12 600) at 56 °C to IF(n=1) crystals. This indicates that the friction coefficient has a smaller effect on the molecular motion in this temperature range. As long as the number of folds are the same, the transition kinetics (the slopes) gradually decreases with increasing molecular weight. Similar observations hold for the isothermal thickening processes. On the other hand, it is evident that, with increasing the fold number, the transition kinetics diminishes as listed in Table II.

Conclusion

Low molecular weight PEO fractions serve as a bridge for the understanding of polymer crystallization which was originally extended from the crystallization of small molecules. An interesting feature of the crystallization is the initial growth of NIF crystals in these fractions, followed by an isothermal thickening or thinning process to form IF crystals. The unique observation of the isothermal thinning process is critically dependent upon the thermodynamic stability of NIF crystals, which is associated not only with fold length but also with chain end defects within the crystals, as well as the nature of the chain fold surface. The fold length of NIF crystals is proportional to the reciprocal of the supercooling for each fraction as predicted by nucleation theory, but the slopes of these linear relationships are different. The detailed kinetics of isothermal thickening and thinning processes illustrate the effects of chain diffusion distance along the c-axis and chain fold number. With increasing molecular weight, these processes are increasingly forbidden, and NIF crystals may remain permanently as a final metastable crystalline state.

Acknowledgment. This research was partially supported by the Exxon Education Foundation. S.Z.D.C. gratefully acknowledges the support of his Presidential Young Investigator Award (DMR 91-57738) from the National Science Foundation. Research was carried out (in part) at the National Synchrotron Light Source (NSLS), Brookhaven National Laboratories, which is supported by the U.S. Department of Energy, Division of Materials Sciences and Division of Chemical Sciences.

References and Notes

(1) Kovacs, A. J.; Gonthier, A. *Kolloid Z. Z. Polym.* **1972**, *250*, 530.
(2) Kovacs, A. J.; Gonthier, A.; Straupe, C. *J. Polym. Sci., Polym. Symp.* **1975**, *50*, 283.
(3) Kovacs, A. J.; Straupe, C.; Gonthier, A. *J. Polym. Sci., Polym. Symp.* **1977**, *59*, 31.
(4) Kovacs, A. J.; Straupe, C. *Faraday Discuss. Chem. Soc.* **1979**, *68*, 225.
(5) Kovacs, A. J.; Straupe, C. *J. Cryst. Growth* **1980**, *48*, 210.
(6) Hartley, A.; Leung, Y. K.; Booth, C.; Shepherd, I. W. *Polymer* **1976**, *17*, 354.
(7) Fraser, M. J.; Marshall, A.; Booth, C. *Polymer* **1977**, *18*, 93.
(8) Ashman, P. C.; Booth, C. *Polymer* **1973**, *14*, 300.
(9) Ungar, G.; Keller, A. *Polymer* **1986**, *27*, 1835.
(10) Ungar, G.; Keller, A. *Polymer* **1987**, *28*, 1899.
(11) Organ, S. J.; Ungar, G.; Keller, A. *Macromolecules* **1989**, *22*, 1995.
(12) Cheng, S. Z. D.; Zhang, A.-Q.; Chen, J.-H. *J. Polym. Sci., Polym. Lett. Ed.* **1990**, *28*, 233.
(13) Cheng, S. Z. D.; Zhang, A.-Q.; Chen, J.-H.; Heberer, D. P. *J. Polym. Sci., Polym. Phys. Ed.* **1991**, *29*, 287.
(14) Cheng, S. Z. D.; Chen, J.-H.; Zhang, A.-Q.; Heberer, D. P. *J. Polym. Sci., Polym. Phys. Ed.* **1991**, *29*, 299.
(15) Cheng, S. Z. D.; Chen, J.-H. *J. Polym. Sci., Polym. Phys. Ed.* **1991**, *29*, 311.
(16) Cheng, S. Z. D.; Zhang, A.-Q.; Barley, J. S.; Chen, J.-H.; Habenschuss, A.; Zschack, P. R. *Macromolecules* **1991**, *24*, 3937.
(17) Cheng, S. Z. D.; Chen, J.-H.; Zhang, A.-Q.; Barley, J. S.; Habenschuss, A.; Zschack, P. R. *Polymer*, in press.
(18) Buckley, C. P.; Kovacs, A. J. *Prog. Colloid Polym. Sci.* **1975**, *58*, 44.
(19) Buckley, C. P.; Kovacs, A. J. *Colloid Polym. Sci.* **1976**, *254*, 695.
(20) Habenschuss, A.; Ice, G. E.; Sparks, C. J.; Neiser, R. A., Jr. *Nucl. Instrum. Methods* **1988**, *A266*, 215.
(21) Chen, J.-H. Ph.D. Dissertation, Department of Polymer Science, University of Akron, Akron, OH, 1992.
(22) Cheng, S. Z. D.; Barley, J. S.; Giusti, P. A. *Polymer* **1990**, *31*, 845.
(23) Phillips, P. J.; Rensch, G. J. *J. Polym. Sci., Polym. Phys. Ed.* **1989**, *27*, 155.
(24) Song, K.; Krimm, S. *Macromolecules* **1990**, *23*, 1946.
(25) Lauritzen, J. I.; Jr.; Hoffman, J. D. *J. Appl. Phys.* **1973**, *44*, 4340.
(26) Hoffman, J. D.; Davis, G. T.; Lauritzen, J. I., Jr. In *Treatise on Solid State Chemistry*; Hannay, N. B., Ed.; Plenum: New York, 1976; Vol. 3, Chapter 7, pp 497–614.
(27) Hoffman, J. D. *Polymer* **1982**, *23*, 656.
(28) Hoffman, J. D. *Macromolecules* **1986**, *19*, 1124.
(29) Hoffman, J. D.; Miller, R. L. *Macromolecules* **1988**, *21*, 3038.
(30) Buckley, C. P. *Polymer* **1980**, *21*, 444.
(31) Sadler, D. M. *J. Polym. Sci., Polym. Phys. Ed.* **1985**, *23*, 1533.
(32) Lauritzen, J. I., Jr.; Passaglia, E. *J. Res. Natl. Bur. Stand., Sect. A* **1967**, *71A*, 261.
(33) Hoffman, J. D.; Frolen, L. J.; Ross, G. S.; Lauritzen, J. I., Jr. *J. Res. Natl. Bur. Stand., Sect. A* **1975**, *79A*, 671.
(34) Cheng, S. Z. D.; Chen, J.-H.; Heberer, D. P. *Polymer*, in press.
(35) Barham, P. J.; Keller, A. *J. Polym. Sci., Polym. Phys. Ed.* **1989**, *27*, 1029.